eNeuro

Research Article: New Research | Disorders of the Nervous System

Posttraumatic stress disorder is associated with alpha dysrhythmia across the visual cortex and the default mode network

https://doi.org/10.1523/ENEURO.0053-20.2020

Cite as: eNeuro 2020; 10.1523/ENEURO.0053-20.2020

Received: 13 February 2020
Revised: 15 June 2020
Accepted: 19 June 2020

Posttraumatic stress disorder is associated with alpha dysrhythmia across the visual cortex and the default mode network

Abbreviated title: **Visual-cortex-DMN alpha dysrhythmia in PTSD**

Kevin J. Clancy, M.S.[1], Jeremy A. Andrzejewski, M.S. [1], Jessica Simon, B.A., Mingzhou Ding, Ph.D. [2], Norman B. Schmidt, Ph.D. [1], & Wen Li, Ph.D. [1]

[1] Department of Psychology, Florida State University, Tallahassee, FL, 32304

[2] J. Crayton Pruitt Family Department of Biomedical Engineering, University of Florida, Gainesville, FL, 32611

Correspondence concerning this article should be addressed to Wen Li (wenli@psy.fsu.edu) and Kevin Clancy (clancy@psy.fsu.edu), Department of Psychology, Florida State University, B342 PDB, 1107 W. Call St., Tallahassee, FL 32303.

Word count Abstract: 248

Word count Introduction: 748

Word count Discussion: 1734

Number of Figures: 4

Number of Tables: 3

Key words: posttraumatic stress disorder; default mode network; alpha oscillations; sensory disinhibition; resting-state

Acknowledgement and Funding sources: This research was supported by the National Institute of Mental Health grants R01MH093413 (W.L.), the FSU Chemical Senses Training (CTP) Grant Award T32DC000044 (K.C.) from the National Institutes of Health (NIH/NIDCD), and the Subaward of U.S. Army award W81XWH-10-2-018 (N.S.), which does not necessarily represent the views of the Department of Defense, Department of Veterans Affairs, or the United States Government, nor does it constitute or imply endorsement, sponsorship, or favoring of the study design, analysis, or recommendations.

Conflicts of Interest: The authors declare no competing financial interests or potential conflicts of interest.

Posttraumatic stress disorder is associated with alpha dysrhythmia across the visual cortex and the default mode network

ABSTRACT

Anomalies in default mode network (DMN) activity and alpha (8-12 Hz) oscillations have been independently observed in posttraumatic stress disorder (PTSD). Recent spatiotemporal analyses suggest that alpha oscillations support DMN functioning via inter-regional synchronization and sensory cortical inhibition. Therefore, we examined a unifying pathology of alpha deficits in the visual-cortex-DMN system in PTSD. Human patients with PTSD ($N = 25$) and two control groups—patients with Generalized Anxiety Disorder (GAD; $N = 24$) and healthy controls (HC; $N = 20$)—underwent a standard eyes-open resting state (S-RS) and a modified resting state (M-RS) of passively viewing salient images (known to deactivate the DMN). High-density electroencephalogram (hdEEG) were recorded, from which intracortical alpha activity (power and connectivity/Granger causality) was extracted using the exact low-resolution electromagnetic tomography (eLORETA). Patients with PTSD (vs. GAD/HC) demonstrated attenuated alpha power in the visual cortex and key hubs of the DMN (posterior cingulate cortex/PCC and medial prefrontal cortex/mPFC) at both states, the severity of which further correlated with hypervigilance symptoms. With increased visual input (at M-RS vs. S-RS), patients with PTSD further demonstrated reduced alpha-frequency directed connectivity within the DMN (PCC→mPFC) and, importantly, from the visual cortex (VC) to both DMN hubs (VC→PCC and VC→mPFC), linking alpha deficits in the two systems. These interrelated alpha deficits align with DMN hypoactivity/hypoconnectivity, sensory disinhibition, and hypervigilance in PTSD, representing a unifying neural underpinning of these anomalies. The

identification of visual-cortex-DMN alpha dysrhythmia in PTSD further presents a novel therapeutic target, promoting network-based intervention of neural oscillations.

SIGNIFICANCE STATEMENT

Alpha (8-12 Hz) oscillations and the default mode network (DMN) both dominate the resting-state brain activity and are found to be closely related. In addition, aberrant alpha and DMN activities are both implicated in the pathophysiology of posttraumatic stress disorder (PTSD). Linking alpha and DMN aberrations in PTSD, our high-density EEG source analysis reveals that PTSD is associated with alpha power deficits across the DMN and visual cortex (VC) and deficient alpha-frequency connectivity from the VC to the DMN. That this visual-cortex-DMN alpha dysrhythmia further underpins hypervigilance symptoms in PTSD highlights a temporal-spatial network pathology, promoting network-based neural oscillatory interventions.

INTRODUCTION

Prevailing models of the neuropathology of posttraumatic stress disorder (PTSD) have focused on dysfunctions of the prefrontal-cortex-amygdala circuit (Rauch et al., 2006; Liberzon and Abelson, 2016). Recently, evidence has extended this circuit pathology to implicate large-scale brain network anomalies (Spielberg et al., 2015; Koch et al., 2016; Liberzon and Abelson, 2016; Akiki et al., 2017). Anomalies in the default mode network (DMN), a major resting-state network (RSN), have been especially highlighted in this literature, characterized by attenuated network activity and disrupted network communication (Bluhm et al., 2009; Lanius et al., 2010; Sripada et al., 2012; Koch et al., 2016; Akiki et al., 2018).

The DMN is one of the most consistently identified RSNs, anchored in a midline core consisting of two key hub structures—the posterior cingulate cortex (PCC) and the medial prefrontal cortex (mPFC) (Buckner et al., 2008; Yeo et al., 2011). While prominent in the resting state, the DMN is deactivated by salient sensory input or externally-oriented cognitive processing and, accordingly, exhibits reciprocal inhibition with neural networks associated with these processes (Gusnard et al., 2001; Raichle et al., 2001; Greicius et al., 2003; Greicius and Menon, 2004). As such, DMN dysfunctions can interrupt internal mentation or 'tranquil' resting states and heighten vigilance and attention. Indeed, DMN dysfunction has been linked to heightened acute stress response (Menon, 2011; Hermans et al., 2014; Zhang et al., 2019) and implicated in PTSD symptoms of hypervigilance and negative intrusions (Abdallah et al., 2017; Akiki et al., 2018).

While neuroimaging data have isolated the DMN as the dominant network in the resting brain, electrophysiological data have identified alpha (8-12 Hz) oscillations as the dominant electrical activity in the resting brain (Klimesch et al., 2007; Klimesch, 2012). Alpha oscillations represent a neural mechanism mediating long-range inter-regional interactions (Palva and Palva,

2007; Tang et al., 2007; Hillebrand et al., 2016). Importantly, evidence has begun to link alpha oscillations to DMN activity (especially during eyes-open resting state) (Mantini et al., 2007; Jann et al., 2009; Knyazev et al., 2011; Scheeringa et al., 2012; Mo et al., 2013), raising the possibility that, to some extent, the DMN could be organized and maintained by long-range synchronization of alpha oscillations (Engel and Singer, 2001; Uhlhaas et al., 2008; Jann et al., 2009).

While alpha oscillations positively correlate with DMN activity, they are known to negatively correlate with visual cortical activity (Klimesch et al., 2007; Jensen and Mazaheri, 2010; Lange et al., 2013). Alpha oscillations (originating in the sensory cortex and thalamus) play a key role in visual inhibition by suppressing cortical excitation and feedforward propagations (Klimesch et al., 2007; Palva and Palva, 2007; Tang et al., 2007; Jensen and Mazaheri, 2010; Foxe and Snyder, 2011; Klimesch, 2012; Hillebrand et al., 2016; Johnson et al., 2017). This active function of alpha oscillations can present a second mechanism—visual cortical inhibition—to support DMN activity. That is, by suppressing visual processing, alpha oscillations could protect the DMN from environmental disruptions.

Alternatively, deficient alpha activity could give rise to DMN dysfunctions by failing to sustain long-range synchronization across the DMN and failing to inhibit sensory afferents to the DMN. Aberrant alpha oscillations have been featured in a “thalamocortical dysrhythmia” model of neuropsychiatric disorders (Llinas et al., 1999; Schulman et al., 2011), which are conceptualized transdiagnostically as oscillopathies (Basar, 2013; Buzsaki et al., 2013). Reduced resting-state alpha activity has been observed in patients with PTSD (vs. healthy controls and patients with generalized anxiety disorder/GAD) (Clancy et al., 2017) and combat veterans with severe symptoms (Clancy et al., 2020). Given the demonstrated association between alpha

oscillations and DMN activity, we hypothesized that PTSD is associated with deficient alpha activity in the DMN and deficient inhibition of sensory cortical input to the DMN.

Therefore, by extracting intracortical alpha activity from high-density electroencephalogram (EEG) recordings, we conducted source-level analysis of resting-state alpha activity in patients with PTSD, relative to healthy controls and patients with GAD. The GAD group was included to rule out effects of general anxiety and hyperarousal that would confound resting-state neural oscillations (Imperatori et al., 2019). For simplicity and statistical rigor, the GAD group and healthy control group were collapsed into a single Control group, which was further justified by prior work by Clancy et al. demonstrating a lack of surface-level differences between HC and GAD groups (Clancy et al., 2017). Comparisons between PTSD and HC or GAD groups separately are also reported. To highlight the vulnerability of the DMN to sensory input, we included a modified resting state (M-RS) involving passive viewing of images, in addition to a standard, eyes-open resting state (S-RS). We assessed two specific hypotheses of alpha deficits in PTSD, including (1) attenuated alpha power and connectivity in the DMN and (2) a deficit of alpha inhibition of visual cortical (VC) activity (i.e., attenuated alpha power) and attenuated directed alpha-frequency connectivity to the DMN (VC→DMN). Finally, we hypothesized that deficient sensory inhibition could be associated with the PTSD symptom of hypervigilance (characterized by excessive sensory scanning of the environment for threat) and thus examined these clinical associations, linking neuropathology to clinical symptomatology.

METHODS & MATERIALS

Participants

Participants consisted of outpatients with a current diagnosis of PTSD ($N = 25$) or GAD ($N = 24$), and healthy controls (HC; $N = 20$) with no current or past-year diagnoses. Participants were matched for age and gender across groups. Participants were recruited through community advertisement as part of a larger randomized controlled trial and compensated monetarily for their participation in the study. Inclusion criteria were primary diagnoses of PTSD or GAD, respectively, or no current or past-year psychiatric disorders for the healthy control (HC) group. Participants with co-morbid diagnoses of PTSD and GAD were excluded. Participants were further excluded based on the following criteria: history of suspected severe TBI (i.e., exceeding 30 minutes of loss of consciousness due to a head or neck injury), history of neurological disorders, and diagnosis of psychotic disorders, severe substance use disorder, or abuse of opioids, stimulants, or cocaine. 6 PTSD participants met diagnostic criteria for mild alcohol use disorder (n = 3) or mild cannabis use disorder (n = 3). 32% of Controls (GAD $n = 7$, HC $n = 7$) had a history of a DSM-5 Criterion A trauma. Index trauma types of participants with PTSD ranged from combat exposure ($n = 6$), vehicular accident ($n = 3$), rape ($n = 7$), and sexual ($n = 5$) or physical assault ($n = 4$). 48% ($n = 12$) of participants in the PTSD group reported multiple traumas. The mean number of traumas in the PTSD group was 4.22 (+/- 2.26). All participants provided written, informed consent to participate in the study, which was approved by both the university's Institutional Review Board and the Department of Defense Human Research Protection Official's Review. Demographic details are presented in Table 1.

Clinical Assessment

Current or past-year diagnoses were assessed by trained clinicians using the Structured Clinical Interview for DSM-5 (American Psychiatric Association, 2013). Participants

additionally completed the PTSD Checklist for DSM-IV: civilian version (Blanchard et al., 1996). In the present study, internal consistency was high for the total questionnaire ($\alpha = 0.95$) and the hyperarousal subscale ($\alpha = 0.84$). As in previous work (Mueller-Pfeiffer et al., 2013; Clancy et al., 2017), Item 16 assessing symptoms of hypervigilance or 'being watchful or on guard' was extracted to index hypervigilance.

Experimental Paradigm

Participants were seated in a comfortable recliner in a dimly lit, sound attenuated and electrically shielded room. High-density electroencephalogram (EEG) data were recorded during two resting states. To evaluate intrinsic neural activity, a standard resting state (S-RS) recording was conducted first, lasting 2 minutes while participants fixated on a crosshair on the screen. To assess the impact of environmental sensory input on alpha oscillations and DMN functioning, a modified resting state (M-RS) recording was also conducted, involving 5 minutes of passively viewing a continuous stream of images (subtending a visual area of 7.8° X 5.8°), each for 333 ms. Images were chosen from the International Affective Picture System (Lang et al., 2008), depicting neutral (e.g. buildings, daily objects; n = 322), positive (e.g. erotic; n = 253), and negative (e.g. mutilation; n =346) scenes, randomly intermixed.

EEG Acquisition and Preprocessing

EEG data were recorded from a 96 channel BrainProducts actiCap system with Neuroscan SynAmps RT amplifiers (1000 Hz sampling rate, 0.05-200 Hz online bandpass filter, referenced to the FCz channel). Electro-oculogram (EOG) was recorded using four electrodes with vertical and horizontal bipolar derivations. EEG/EOG data were downsampled to 250 Hz,

high-pass (1 Hz) and notch (60 Hz) filtered. We then applied *Fully Automated Statistical Thresholding for EEG artifact Rejection* algorithm (FASTER) (Nolan et al., 2010) for artifact detection, correction, and rejection. Output data were epoched into 1-second segments and submitted to eLORETA for source analyses.

Exact low-resolution electromagnetic tomography (eLORETA)

Using the high-density, artifact-minimized EEG data, we conducted intracranial source analyses using eLORETA, a linear inverse solution to reconstruct cortical activity with scalp EEG data (Pascual-Marqui et al., 2011). The LORETA algorithm has been cross-validated in multiple studies combining EEG-based LORETA with fMRI (Worrell et al., 2000; Vitacco et al., 2002; Mulert et al., 2004; Mobascher et al., 2009; Olbrich et al., 2009), positron emission tomography (Dierks et al., 2000; Pizzagalli et al., 2004), and intracranial recordings (Zumsteg et al., 2005). The solution space consists of 6239 cortical gray matter voxels with a spatial resolution of 5 x 5 x 5 mm in a realistic head model. eLORETA is a suitable tool to investigate network activity and connectivity (Neuner et al., 2014; Thatcher et al., 2014; Liu et al., 2017; Samogin et al., 2019) and has provided important network insights into psychiatric disorders (Whitton et al., 2018; Imperatori et al., 2019; Samogin et al., 2019).

For accurate inverse solutions, eLORETA was modeled for the S-RS and M-RS separately, from which whole-brain source estimates of alpha (8-12 Hz) power were derived (Pascual-Marqui et al., 2011). For source-based alpha-frequency connectivity analysis, time series of regions of interest were derived from eLORETA (Samogin et al., 2019), which were then submitted to Granger causality analysis based on bivariate autoregressive (AR) modelling (Ding et al., 2006). A model order of 20 (80 ms in time for a sampling rate of 250 Hz) was

chosen in a two-step process: (1) Akaike Information Criterion (AIC) and (2) comparing spectral estimates obtained by the Fourier-based AR model for data pooled across all subjects (Wang et al., 2016). Our focus on the alpha frequency was guided by *a priori* hypotheses stemming from 1) the purported role of alpha oscillations in the sensory disinhibition model of PTSD and 2) prior work by Clancy et al. demonstrating no surface-level effects of PTSD-related aberrations in neighboring theta or beta frequencies (p's > 0.16) (Clancy et al., 2017).

Regions of Interest (ROIs): DMN hubs (i.e., PCC and mPFC) and visual cortex were selected as ROIs (Yeo et al., 2011; Tamber-Rosenau et al., 2013). ROIs were defined by grey-matter voxels within a 10 mm radius of the ROI centroids (Pascual-Marqui et al., 2011; Whitton et al., 2018). All ROIs were centered on the midline to incorporate both hemispheres, with centroid coordinates obtained from the Neurosynth (www.neurosynth.org) meta-analysis maps (as peak voxels) of "default mode" (for the PCC: 0, -50, 30 and the mPFC: 0, 50, 0) and "passive viewing" (for the visual cortex: 0, -90, 20). All coordinates are reported in Montreal Neurological Institute (MNI) space. For connectivity analysis, both directions for each pair were examined such that the three ROIs resulted in a 3 x 3 matrix of alpha-GC connectivity for each of the two resting states.

Statistical Analyses

Source-level power and GC were submitted to planned simple contrasts of States (S-RS vs. M-RS) to demonstrate the extent of alpha adaption from S-RS to M-RS. We then performed simple contrasts of Group (PTSD vs. Control) for the two states to test PTSD-related deficits in alpha power and GC, and double contrasts of State and Group to assess the effect of visual stimulation (S-RS minus M-RS) between groups. Pearson correlations were performed to assess

clinical associations of alpha power and GC with symptom severity of hypervigilance. Guided by previous surface-level analyses showing no difference between the two control groups (GAD and HC) (Clancy et al., 2017), we combined them into a single Control group. Our supplemental analyses confirmed that these two control groups did not differ in source-level alpha activity.

Multiple-comparison corrections were applied for the analyses. For power analyses involving whole-brain voxel-wise comparisons, we used Monte Carlo simulations (with actual Gaussian filter widths extracted from the data) to derive the corrected threshold ($p < .05$): voxel level $p < 0.005$ (one-tailed) over eleven contiguous voxels. As for connectivity analyses, the 3 x 3 connectivity matrix resulted in 6 comparisons for each hypothesis testing, for which we applied the false discovery rate (FDR) criterion (FDR $p < .05$). Lastly, for clinical association analyses, we conducted confirmatory correlation analyses constrained to regions demonstrating main effects, for which correction was not applied. We also applied a whole-brain regression of alpha power on hypervigilance scores, followed by Monte Carlo multiple comparison correction. While the sensory hypothesis implicates a direct association between sensory disinhibition and hypervigilance symptoms, it is possible that this sensory pathology also contributes to other PTSD symptom clusters. However, correlations between reduced source-level alpha power and total PCL scores (S-RS/M-RS r's > -0.10/-0.14, p's > 0.41/0.25) or other subscale scores (r's > -0.16; p's > 0.19) indicate rather weak effects. We thus focused on the hypervigilance symptoms below. Trend-level and non-corrected effects will be reported but not further discussed.

RESULTS

PTSD-related alpha power deficits in the DMN and visual cortex

Validating intracranial source estimation of alpha oscillations, we observed "alpha blocking" by visual stimulation. Specifically, the contrast between S-RS versus M-RS (collapsed across groups) isolated alpha power reduction at M-RS across a large cluster (624 voxels) spanning bilateral visual cortices (peak voxel: -20, -100, 0; t = -4.50, d = 1.09).

Next, simple contrasts of Group (PTSD vs. Controls) revealed alpha power deficits in PTSD across the visual and DMN ROIs at each state. The visual cortex exhibited the strongest group effects: at S-RS, a large cluster (283 voxels) spanning bilateral cuneus (peaks: 5, -70, 30/-5, -70, 30; t's < -3.41, d's > 0.83), bilateral precuneus (peaks: 5, -60, 35/-5, -65, 25; t's < -3.75, d's > 0.92), and the right superior occipital gyrus (peak: 40, -80, 25; t = -3.90, d's > 0.96; Figure 1A); at M-RS, a cluster (68 voxels) in the bilateral precuneus, overlapping the S-RS cluster (peaks: 5, -55, 50/-5, -55, 40; t's < -3.11, d's > 0.76; Figure 1B). Regarding the DMN, alpha deficits emerged in PTSD in the bilateral PCC for both states (S-RS: 60 voxels; peaks: 15, -45, 40/-5, -50, 35; t's < -3.32, d's > 0.81; M-RS: 199 voxels; peaks: 5, -30, 25/-5, -30, 25; t's < -3.76, d's > 0.92; Figure 1A-B), and the bilateral mPFC at M-RS only (88 voxels; peaks: 15, 60, -10/-15, 65, -15; t's < -3.10, d's 0.76; Figure 1B). Additional alpha power deficits (whole-brain corrected) appeared in the bilateral insula (S-RS: right/left: 49/76 voxels; peaks: 35, -5, 20/-35, 20, 5; Figure 1A; M-RS: right/left: 136/25 voxels; peaks: 40, -5, 15/-30, 25, 5; Figure 1B; t's < -3.52, d's = 0.86). No significant clusters emerged for enhanced alpha power in the PTSD group, even at a lenient threshold of p < .05. Finally, double contrasts of State (M-RS minus S-RS) and Group (PTSD minus Control) yielded no difference between groups (voxel-level p's > 0.11). These group effects are summarized in Table 2.

Individual Group contrasts of PTSD vs. GAD or HC separately were then performed to substantiate the PTSD vs. Controls difference. As summarized in Table 3, concerning alpha

power, these contrasts revealed essentially identical results as reported above. Moreover, the effect sizes were comparable (*d*'s = 0.74-1.04) and survived correction for multiple comparisons. In addition, HC and GAD did not differ on any of these contrasts (*p*'s > 0.39).

PTSD-related alpha connectivity deficits within and between the DMN and visual cortex

Like the power analyses above, we first assessed the effect of State (S-RS vs. M-RS) on alpha-frequency connectivity (collapsed across the groups). We observed reduced bidirectional alpha connectivity from the S-RS to the M-RS within the DMN: PCC →mPFC (M-RS minus S-RS; t = -3.49, p = 0.001, FDR p < 0.05, d = 0.85) and mPFC→PCC (t = -3.14, p = 0.003, FDR p < 0.05, d = 0.76), suggesting disrupted DMN connectivity in general by salient visual input (at M-RS).

Next, simple contrasts of Group for the S-RS revealed reduced alpha connectivity from the PCC to the visual cortex/VC (PCC →VC) in PTSD (vs. Controls; t = -2.26, p = 0.027, d = 0.55; Figure 2A), albeit failing FDR correction. No other effects emerged during this state (*p*'s > .34). For the M-RS, the PTSD group (vs. Controls) demonstrated reduced connectivity within the DMN, including PCC →mPFC (t = -2.82, p = .008, FDR p < 0.05, d = 0.69; Figure 2B) and, at a trend level, mPFC→PCC (t = -1.91, p = 0.064, d = 0.47). The PTSD group demonstrated additional deficits in alpha connectivity from the visual cortex to both DMN ROIs at M-RS: VC→PCC (t = -3.06, p = 0.004, FDR p < 0.05, d = 0.75) and VC→mPFC (t = -2.05, p = .049, d = 0.50; albeit not FDR corrected). No effect appeared in the opposite (DMN→VC) direction (*p*'s > 0.12). We further explored whole-brain connectivity with the PCC seed during the M-RS between the PTSD and control groups (Figure 3). At the familywise threshold, correcting for the 84 Brodmann areas examined (FWE p = .0006), only one additional area emerged with

297 attenuated connectivity from the PCC to the right associative auditory cortex (superior temporal
298 gyrus - Brodmann's Area 22; t = -3.93, p = 0.0003) in the PTSD group at MRS. This effect thus
299 aligned with the VC-PCC dysconnectivity in PTSD above.

300 Double contrasts of State (M-RS minus S-RS) and Group (PTSD vs. Control) revealed
301 different effects of state (i.e., visual stimulation) on connectivity between the groups. Greater
302 connectivity reduction from S-RS to M-RS appeared in the PTSD (vs. Control) group in
303 VC→PCC (t = -2.22, p = 0.032, d = 0.54) and VC→mPFC (t = -2.18, p = 0.036, d = 0.53).
304 Specifically, from S-RS to M-RS, significant connectivity reduction emerged in VC→PCC (t = -
305 2.84, p = 0.011, FDR p < 0.05, d = 0.69) and VC→mPFC (t = -3.04, p = 0.007, FDR p < 0.05, d =
306 0.74) in the PTSD group, but none in the Control group (p's > 0.628). These group effects are
307 also summarized in Table 2.

308 Finally, individual Group contrasts were performed to substantiate the PTSD vs. Controls
309 difference. Again, these specific contrasts revealed consistent results to those from the main
310 analyses (Table 3). A notable difference was that, owing to the reduced group size, the
311 PCC→VC deficit in PTSD at S-RS survived one-tailed tests only (PTSD vs. HC: t = -1.72, p =
312 0.046 one-tailed, d = 0.52; vs. GAD: t = -1.83, p = 0.037 one-tailed, d = 0.53), as did the
313 VC→PCC deficit in the double contrast (PTSD vs. HC, t = -1.87, p = 0.034 one-tailed, d = 0.57;
314 PTSD vs. GAD, t = -1.87, p = 0.035 one-tailed, d = 0.55). However, given the strong *a priori*
315 hypothesis of deficient alpha connectivity in PTSD, these tests could provide support to the
316 hypothesis. The double contrast on VC→mPFC alpha connectivity showed a significant deficit
317 in PTSD in comparison to GAD (t = -2.29, p = 0.027, d = 0.67) but only a marginal deficit in
318 comparison to HC (t = -1.50, p = 0.071 one-tailed, d = 0.46).

These group-specific contrasts also revealed additional results: at M-RS, the GAD (vs. PTSD or HC) group demonstrated increased alpha connectivity from mPFC→PCC (GAD vs. PTSD: $t = 3.25$, $p = 0.003$, $d = 0.95$; GAD vs. HC: $t = 2.65$, $p = 0.012$, $d = 0.82$), suggesting GAD-specific augmentation in this alpha connectivity. No other differences emerged between the HC and GAD groups (p's > 0.411).

Clinical Associations

We then performed correlation analyses, regressing power or connectivity values on symptom severity in hypervigilance. Confirmatory analyses (constrained to the regions identified in the main contrasts) revealed negative associations between hypervigilance and alpha power in the precuneus/superior parietal lobule at S-RS (39 voxels; peak: -20, -75, -55; $r = -0.49$, $p < .005$; Figure 4A) and the DMN at M-RS: PCC (13 voxels; peak: 5, -45, 45; $r = -0.28$, $p < .05$) and mPFC (50 voxels; peak: -10, 65, -15; $r = -0.30$, $p < .05$; Figure 4B). Whole-brain regression analysis further revealed negative associations with alpha power in the ventral visual cortex at S-RS (left inferior temporal gyrus: 13 voxels; peak: -55, -5, -40; $r = -0.40$, $p < .005$ whole-brain corrected; Figure 4A). There was no significant correlation between hypervigilance and alpha connectivity (p's > 0.20).

DISCUSSION

Source-level analysis of RS alpha oscillations isolated alpha (power and connectivity) deficits in the DMN and visual cortex in PTSD, especially during strong visual stimulation. In support of our first hypothesis — alpha deficits in the DMN, the PTSD group demonstrated reduced alpha power in the posterior DMN hub (the PCC) at both S-RS and M-RS as well as the

342 anterior hub (the mPFC) at M-RS, accompanied by reduced DMN (PCC→mPFC) alpha-
343 frequency connectivity at M-RS. In support of the second hypothesis — alpha deficits in the
344 visual cortex, the PTSD group exhibited reduced alpha power in the visual cortex at both states.
345 Importantly, joining alpha deficits in the two neural systems, diminished alpha-frequency
346 connectivity from the visual cortex to the DMN was observed in the PTSD group at M-RS.
347 Finally, alpha power deficits in the DMN and visual cortex directly correlated with symptom
348 severity of hypervigilance. Therefore, linking anomalies in DMN and alpha activity in PTSD, the
349 current results indicate interrelated alpha deficits in the DMN and visual cortex, implicating
350 visual-cortex-DMN alpha dysrhythmia in the neuropathology of PTSD.

351 Neural oscillations actively participate in mental activities by modulating local neuronal
352 excitability and mediating long-range neural communication (Buzsaki and Draguhn, 2004;
353 Buzsaki et al., 2013). Aberrant resting-state (intrinsic) neural oscillations (e.g., thalamocortical
354 dysrhythmia) in neuropsychiatric disorders has been increasingly recognized (Llinas et al., 1999;
355 Schulman et al., 2011; Vanneste et al., 2018), promoting the transdiagnostic conceptualization of
356 "oscillopathies" for these disorders (Basar, 2013; Buzsaki et al., 2013). Advancements in neural
357 computational algorithms (such as eLORETA) have permitted intracranial source estimation of
358 neural oscillations in hdEEG recordings, providing important insights into oscillatory
359 dysrhythmia in multiple disorders, e.g., schizophrenia (Canuet et al., 2011; Di Lorenzo et al.,
360 2015), depression (Whitton et al., 2018), and PTSD (Imperatori et al., 2014). As validation of our
361 hdEEG source analysis, we confirmed a strong "alpha blocking" effect of visual stimulation by
362 demonstrating extensive alpha power reduction in bilateral visual cortices from the S-RS
363 (minimal visual input) to the M-RS (strong visual input). By contrast, no other regions emerged

from this contrast, highlighting the sensitivity and specificity of this source analysis of alpha oscillations.

Our source-level group analysis further identified alpha deficits within and between the visual cortex and the DMN in PTSD. Concerning the visual cortex, alpha oscillations are known to mediate visual cortical inhibition, and accordingly, alpha power correlates inversely with visual cortical activity (Klimesch et al., 2007; Palva and Palva, 2007; Jensen and Mazaheri, 2010; Lange et al., 2013). In the PTSD group, reduced alpha power in the visual cortex was extensive and enduring across states. Without visual stimulation (at S-RS, reflecting intrinsic activity), alpha deficits spanned a large cluster over the cuneus, precuneus, and superior occipital gyrus, suggesting wide-spread, intrinsic neural disinhibition and hyperactivity across primary and secondary visual cortices in PTSD. This sensory cortical disinhibition aligns with extant electrophysiological evidence of impaired sensory gating and sensory cortical hyperactivity (to simple, neutral stimuli) (Morgan and Grillon, 1999; Neylan et al., 1999; Stewart and White, 2008; Javanbakht et al., 2011) and behavioral disturbances in sensory filtering/gating and response in these patients (Stewart and White, 2008; Engel-Yeger et al., 2013). With strong visual input at M-RS, alpha power reduction was particularly localized to the parietal visual cortex (primarily bilateral precuneus). Given that this region is strongly involved in visual spatial attention and perception (Corbetta et al., 1995; Behrmann et al., 2004; Corbetta and Shulman, 2011) and that the M-RS condition mimics a real-life environment with salient sensory information, this alpha deficit (reflective of disinhibited visual spatial attention) can underlie hypervigilance in PTSD, expressed as excessive alertness to and scanning of the environment (Conoscenti et al., 2009).

As mentioned above, alpha oscillations also play a role in long-range neural communication and resting-state alpha power correlates positively with DMN activity (Mantini et al., 2007; Jann et al., 2009; Sadaghiani et al., 2010; Knyazev et al., 2011; Mo et al., 2013; Samogin et al., 2019). The alpha deficits in DMN hubs thus dovetails the extant literature citing both deficient alpha activity (Clancy et al., 2017; Clancy et al., 2020) and DMN hypoactivity in PTSD (Koch et al., 2016; Akiki et al., 2018). Notably, resting-state beta and theta oscillations have also been found to be associated with DMN activity (Laufs et al., 2003; Mantini et al., 2007; Scheeringa et al., 2012). However, prior sensor-level analyses have not revealed PTSD-related anomalies in the beta or theta frequencies (p's > 0.16) (Clancy et al., 2017). Future research is warranted to examine the other oscillatory activities in various states or tasks to elucidate their contribution to PTSD pathology.

The fact that DMN alpha power reduction extended from the PCC only at S-RS to both the PCC and mPFC at M-RS accentuates the particular DMN vulnerability in PTSD in a sensory-rich environment. In addition, as alpha oscillations synchronize activity and facilitate coherence across regions, reduced alpha power in these key DMN hubs could further suggest compromised communication across the network in PTSD. Indeed, connectivity analyses revealed reduced PCC→mPFC alpha connectivity at M-RS in the PTSD group. This hypo-connectivity between the DMN hubs highlights impaired communication within the core architecture of the DMN. Clinically, DMN alpha deficits in both local power and inter-hub connectivity, especially acute in a sensory-rich environment, could contribute to difficulty in maintaining "tranquility" or "rest" (Buckner et al., 2008; Abdallah et al., 2017; Akiki et al., 2018) and avoidance of sensory stimulation in patients with PTSD (Stewart and White, 2008; Engel-Yeger et al., 2013).

Our manipulation of visual stimulation between the two states revealed a direct link between alpha deficits in the visual cortex and the DMN. Consistent with general DMN susceptibility to salient sensory input, we confirmed a general reduction (in the entire sample) in bidirectional alpha connectivity between the DMN hubs (PCC→mPFC and mPFC→PC) as visual input increased from the S-RS to the M-RS. Beyond that, in the PTSD (but not Control) group, increased visual stimulation (from S-RS to M-RS) further diminished visual cortical alpha connectivity to both DMN hubs (VC→PCC and VC→mPFC). As mentioned above, alpha oscillations in the sensory cortex mediate sensory inhibition, such that this VC→DMN alpha projection would serve to protect the DMN by blocking sensory afferents to the network. This notion is supported by prior work demonstrating a modulatory role of alpha oscillations in the connectivity within the sensory (visual) cortex and between the visual cortex and DMN hubs (Scheeringa et al., 2012). While this protective inhibitory process withstood the increased visual input at M-RS in the Control group, it broke down among patients with PTSD, suggesting impaired gating of sensory entry to (i.e., compromised protection of) the DMN. Exploratory correlation analyses further indicated a close correlation between VC→PCC and PCC→mPFC alpha connectivity at M-RS ($r = 0.31$, $p = 0.013$), highlighting a mechanistic link between these two pathways. That is, disinhibited visual cortical propagation to the PCC, in the presence of strong environmental input, could further impair PCC-driven alpha synchronization with the mPFC, worsening DMN dysfunction in PTSD. Finally, to rule out the alternative explanation that emotional content (beyond visual stimulation) could contribute to the M-RS effects, we compared RS EEG data acquired before and after 5-minute presentation of negative IAPS pictures from an independent sample of healthy individuals ($N = 45$). There was no change in alpha GC ($t = 0.032$, $p = 0.974$), suggesting that in the absence of visual stimulation, simple

affective effects would not result in alpha connectivity change. Nonetheless, we cannot fully exclude the combined effects of emotion and visual stimulation. That is, the emotional content of visual stimuli may influence alpha GC differently among the three groups. Future studies are warranted to isolate the simple effects of visual stimulation by including neutral images alone.

Together, current findings implicate a core visual-cortex-DMN system of alpha dysrhythmia in PTSD. The critical role of visual cortical alpha deficits in this pathology lends credence to a sensory hypothesis of PTSD centered on sensory cortical disinhibition (Clancy et al., 2017; Li, 2019; Clancy et al., 2020) and bottom-up accounts of PTSD in general (Nicholson et al., 2017; Badura-Brack et al., 2018). Childhood trauma, a common PTSD risk factor, has been associated with various aberrations in the sensory cortex and sensory pathway (Teicher et al., 2016), adding to the support for this sensory hypothesis. Indeed, 36% of the current PTSD sample reported childhood trauma. That said, the means (and standard deviations) of alpha power and connectivity were highly comparable between the childhood trauma subgroup and the rest of the PTSD group, implicating this sensory pathology across trauma types.

This core visual-cortex-DMN system of alpha dysrhythmia was reinforced by the specificity of alpha deficit sources. Despite the use of whole-brain analyses, group differences in alpha power and clinical associations between alpha power and hypervigilance were localized to the visual cortex and the DMN only (except for the associative auditory cortex and insula as discussed below). While DMN hypoactivity is known to be associated with PTSD symptom severity (Sripada et al., 2012; Miller et al., 2017a; Miller et al., 2017b; Akiki et al., 2018), the clinical association in the visual cortex highlights an additional pathway linking visual cortical disinhibition to PTSD symptoms. Notably, the associations with hypervigilance implicate not only both the dorsal (i.e., the parietal cortex) and ventral visual cortices (i.e., the inferior

454 temporal gyrus) but also the higher-order regions with strong interactions with limbic and frontal
455 regions. As the ventral visual cortex underpins visual object perception, its involvement here
456 aligns with the fact that hypervigilance in PTSD is associated with hyperactivity and
457 hypersensitivity to (threat and neutral) sensory cues (Ehlers and Clark, 2000; Hayes et al., 2012),
458 in addition to exessive spatial scanning engaging the dorsal visual cortex. In light of the "sentinel
459 hypothesis" implicating the DMN in sustained monitoring of the environment (i.e., sensory
460 vigilance) (Buckner et al., 2008; Andrews-Hanna, 2012), we surmise this visual-cortex-DMN
461 alpha dysrhythmia in PTSD may fuse the impairment in "sentinel" function (of the DMN) and in
462 sensory cortical inhibition (via alpha oscillations), resulting in a pathological state
463 hypervigilance.

464 While the insula was not an *a priori* ROI in the current study, expansive alpha deficits
465 spanning the posterior and anterior insula emerged in PTSD following whole-brain correction.
466 The insula is a highly heterogeneous structure, with the posterior portion receiving strong
467 sensory afferents and the anterior portion densely connected with limbic and prefrontal regions
468 as a key node of the salience network/SN (Craig, 2002; Critchley, 2004; Seeley et al., 2007;
469 Menon and Uddin, 2010). Abnormal insular and SN activity has been repeatedly observed in
470 patients with PTSD (Lanius et al., 2015; Koch et al., 2016), and alpha suppression via
471 neurofeedback can increase SN activity (Ros et al., 2013). Our data provide preliminary evidence
472 of insular alpha dysrhythmia in PTSD, potentially underlying some of the insular anomalies.
473 Interestingly, our exploratory whole-brain connectivity analyses further isolated an additional
474 region—the right superior temporal gyrus—showing attenuated connectivity with the DMN (i.e.,
475 PCC) in PTSD. This area represents the associative auditory cortex and a primary source of
476 auditory alpha ("tau") oscillations (Lehtela et al., 1997; Billig et al., 2019). This finding thus

477 further bolsters the pathology of sensory-cortex-DMN alpha dysconnectivity in PTSD, extending
478 beyond our *a priori* focus on the visual cortex to other sensory modalities.

479 We included patients with GAD as an additional control condition to rule out general
480 effects of anxiety and arousal on alpha activity. Previous sensor-level analysis of alpha
481 oscillations revealed no alpha deficits in GAD (Clancy et al., 2017), which directed us to
482 combine patients with GAD and healthy controls into one control group in the source-level
483 analysis. Nonetheless, we systematically explored group-specific effects. While the results
484 essentially echoed the main results, we noticed interesting findings of enhanced DMN
485 (mPFC→PCC) alpha connectivity in GAD at M-RS, in comparison to the PTSD and HC groups.
486 We surmise that this mPFC→PCC hyper-connectivity could heighten DMN functioning in GAD,
487 supporting the hallmark symptoms of self-referential rumination and worry in these patients.

488 Integrative neuroimaging and electrophysiological research have promoted the idea that
489 alpha oscillations sustain and facilitate DMN functioning by synchronizing spontaneous activity
490 across the network and suppressing sensory cortical propagation. Translating these mechanisms
491 to the neuropathology of PTSD, we confirmed interconnected alpha deficits in the DMN and
492 visual cortex in patients with PTSD, which are further associated with symptoms of
493 hypervigilance. Therefore, the current findings provide the first evidence of visual-cortex-DMN
494 alpha dysrhythmia in PTSD, presenting a unifying neural underpinning of sensory disinhibition,
495 DMN dysfunction, and hypervigilance in this disorder. The specification of this alpha
496 dysrhythmia further isolates a novel therapeutic target, promoting network-based interventions
497 (Lanius et al., 2015) using brain stimulation of alpha oscillations (Clancy et al., 2018) in the
498 visual-cortex-DMN system as a new line of treatment for PTSD.

References

Abdallah CG, Southwick SM, Krystal JH (2017) Neurobiology of posttraumatic stress disorder (PTSD): A path from novel pathophysiology to innovative therapeutics. Neurosci Lett 649:130-132.

Akiki TJ, Averill CL, Abdallah CG (2017) A Network-Based Neurobiological Model of PTSD: Evidence From Structural and Functional Neuroimaging Studies. Curr Psychiatry Rep 19:81.

Akiki TJ, Averill CL, Wrocklage KM, Scott JC, Averill LA, Schweinsburg B, Alexander-Bloch A, Martini B, Southwick SM, Krystal JH, Abdallah CG (2018) Default mode network abnormalities in posttraumatic stress disorder: A novel network-restricted topology approach. Neuroimage 176:489-498.

American Psychiatric Association (2013) Diagnostic and statistical manual of mental disorders, 5th Edition. Washington, DC.

Andrews-Hanna JR (2012) The brain's default network and its adaptive role in internal mentation. Neuroscientist 18:251-270.

Badura-Brack A, McDermott TJ, Heinrichs-Graham E, Ryan TJ, Khanna MM, Pine DS, Bar-Haim Y, Wilson TW (2018) Veterans with PTSD demonstrate amygdala hyperactivity while viewing threatening faces: A MEG study. Biol Psychol 132:228-232.

Basar E (2013) Brain oscillations in neuropsychiatric disease. Dialogues Clin Neurosci 15:291-300.

Behrmann M, Geng JJ, Shomstein S (2004) Parietal cortex and attention. Curr Opin Neurobiol 14:212-217.

Billig AJ, Herrmann B, Rhone AE, Gander PE, Nourski KV, Snoad BF, Kovach CK, Kawasaki H, Howard MA, 3rd, Johnsrude IS (2019) A Sound-Sensitive Source of Alpha Oscillations in Human Non-Primary Auditory Cortex. J Neurosci 39:8679-8689.

Blanchard EB, Jones-Alexander J, Buckley TC, Forneris CA (1996) Psychometric properties of the PTSD Checklist (PCL). Behav Res Ther 34:669-673.

Bluhm RL, Williamson PC, Osuch EA, Frewen PA, Stevens TK, Boksman K, Neufeld RW, Theberge J, Lanius RA (2009) Alterations in default network connectivity in posttraumatic stress disorder related to early-life trauma. J Psychiatry Neurosci 34:187-194.

Buckner RL, Andrews-Hanna JR, Schacter DL (2008) The brain's default network: anatomy, function, and relevance to disease. Ann N Y Acad Sci 1124:1-38.

Buzsaki G, Draguhn A (2004) Neuronal oscillations in cortical networks. Science 304:1926-1929.

Buzsaki G, Logothetis N, Singer W (2013) Scaling brain size, keeping timing: evolutionary preservation of brain rhythms. Neuron 80:751-764.

Canuet L, Ishii R, Pascual-Marqui RD, Iwase M, Kurimoto R, Aoki Y, Ikeda S, Takahashi H, Nakahachi T, Takeda M (2011) Resting-state EEG source localization and functional connectivity in schizophrenia-like psychosis of epilepsy. PLoS One 6:e27863.

Clancy K, Ding M, Bernat E, Schmidt NB, Li W (2017) Restless 'rest': intrinsic sensory hyperactivity and disinhibition in post-traumatic stress disorder. Brain 140:2041-2050.

Clancy KJ, Albizu A, Schmidt NB, Li W (2020) Intrinsic sensory disinhibition contributes to intrusive re-experiencing in combat veterans. Sci Rep 10:936.

Clancy KJ, Baisley SK, Albizu A, Kartvelishvili N, Ding M, Li W (2018) Lasting connectivity increase and anxiety reduction via transcranial alternating current stimulation. Soc Cogn Affect Neurosci 13:1305-1316.

Conoscenti L, Vine V, Papa A, Litz B (2009) Scanning for danger: Readjustment to the noncombat environment. Living and surviving in harm's way: A psychological treatment handbook for pre- and post-deployment of military personnel:123-145.

Corbetta M, Shulman GL (2011) Spatial neglect and attention networks. Annu Rev Neurosci 34:569-599.

546 Corbetta M, Shulman GL, Miezin FM, Petersen SE (1995) Superior parietal cortex activation during
547 spatial attention shifts and visual feature conjunction. Science 270:802-805.
548 Craig AD (2002) How do you feel? Interoception: the sense of the physiological condition of the body.
549 Nat Rev Neurosci 3:655-666.
550 Critchley HD (2004) The human cortex responds to an interoceptive challenge. Proc Natl Acad Sci U S A
551 101:6333-6334.
552 Di Lorenzo G, Daverio A, Ferrentino F, Santarnecchi E, Ciabattini F, Monaco L, Lisi G, Barone Y, Di Lorenzo
553 C, Niolu C, Seri S, Siracusano A (2015) Altered resting-state EEG source functional connectivity in
554 schizophrenia: the effect of illness duration. Front Hum Neurosci 9:234.
555 Dierks T, Jelic V, Pascual-Marqui RD, Wahlund L, Julin P, Linden DE, Maurer K, Winblad B, Nordberg A
556 (2000) Spatial pattern of cerebral glucose metabolism (PET) correlates with localization of
557 intracerebral EEG-generators in Alzheimer's disease. Clin Neurophysiol 111:1817-1824.
558 Ding M, Chen Y, Bressler SL (2006) Granger Causality: Basic Theory and Application to Neuroscience. In:
559 Handbook of Time Series Analysis, pp 437-460: Wiley-VCH Verlag GmbH & Co. KGaA.
560 Ehlers A, Clark DM (2000) A cognitive model of posttraumatic stress disorder. Behav Res Ther 38:319-
561 345.
562 Engel-Yeger B, Palgy-Levin D, Lev-Wiesel R (2013) The Sensory Profile of People With Post-Traumatic
563 Stress Symptoms. Occupational Therapy in Mental Health 29:266-278.
564 Engel AK, Singer W (2001) Temporal binding and the neural correlates of sensory awareness. Trends
565 Cogn Sci 5:16-25.
566 Foxe JJ, Snyder AC (2011) The Role of Alpha-Band Brain Oscillations as a Sensory Suppression
567 Mechanism during Selective Attention. Front Psychol 2:154.
568 Greicius MD, Menon V (2004) Default-mode activity during a passive sensory task: uncoupled from
569 deactivation but impacting activation. J Cogn Neurosci 16:1484-1492.
570 Greicius MD, Krasnow B, Reiss AL, Menon V (2003) Functional connectivity in the resting brain: a
571 network analysis of the default mode hypothesis. Proc Natl Acad Sci U S A 100:253-258.
572 Gusnard DA, Akbudak E, Shulman GL, Raichle ME (2001) Medial prefrontal cortex and self-referential
573 mental activity: relation to a default mode of brain function. Proc Natl Acad Sci U S A 98:4259-
574 4264.
575 Hayes JP, Vanelzakker MB, Shin LM (2012) Emotion and cognition interactions in PTSD: a review of
576 neurocognitive and neuroimaging studies. Front Integr Neurosci 6:89.
577 Hermans EJ, Henckens MJ, Joels M, Fernandez G (2014) Dynamic adaptation of large-scale brain
578 networks in response to acute stressors. Trends Neurosci 37:304-314.
579 Hillebrand A, Tewarie P, van Dellen E, Yu M, Carbo EW, Douw L, Gouw AA, van Straaten EC, Stam CJ
580 (2016) Direction of information flow in large-scale resting-state networks is frequency-
581 dependent. Proc Natl Acad Sci U S A 113:3867-3872.
582 Imperatori C, Farina B, Adenzato M, Valenti EM, Murgia C, Marca GD, Brunetti R, Fontana E, Ardito RB
583 (2019) Default mode network alterations in individuals with high-trait-anxiety: An EEG functional
584 connectivity study. J Affect Disord 246:611-618.
585 Imperatori C, Farina B, Quintiliani MI, Onofri A, Castelli Gattinara P, Lepore M, Gnoni V, Mazzucchi E,
586 Contardi A, Della Marca G (2014) Aberrant EEG functional connectivity and EEG power spectra in
587 resting state post-traumatic stress disorder: a sLORETA study. Biol Psychol 102:10-17.
588 Jann K, Dierks T, Boesch C, Kottlow M, Strik W, Koenig T (2009) BOLD correlates of EEG alpha phase-
589 locking and the fMRI default mode network. Neuroimage 45:903-916.
590 Javanbakht A, Liberzon I, Amirsadri A, Gjini K, Boutros NN (2011) Event-related potential studies of post-
591 traumatic stress disorder: a critical review and synthesis. Biol Mood Anxiety Disord 1:5.
592 Jensen O, Mazaheri A (2010) Shaping functional architecture by oscillatory alpha activity: gating by
593 inhibition. Front Hum Neurosci 4:186.

Johnson EL, Dewar CD, Solbakk AK, Endestad T, Meling TR, Knight RT (2017) Bidirectional Frontoparietal Oscillatory Systems Support Working Memory. Curr Biol 27:1829-1835 e1824.

Klimesch W (2012) alpha-band oscillations, attention, and controlled access to stored information. Trends Cogn Sci 16:606-617.

Klimesch W, Sauseng P, Hanslmayr S (2007) EEG alpha oscillations: the inhibition-timing hypothesis. Brain Res Rev 53:63-88.

Knyazev GG, Slobodskoj-Plusnin JY, Bocharov AV, Pylkova LV (2011) The default mode network and EEG alpha oscillations: an independent component analysis. Brain Res 1402:67-79.

Koch SB, van Zuiden M, Nawijn L, Frijling JL, Veltman DJ, Olff M (2016) Aberrant Resting-State Brain Activity in Posttraumatic Stress Disorder: A Meta-Analysis and Systematic Review. Depress Anxiety 33:592-605.

Lang P, Bradley M, Cuthbert BN (2008) International affective picture system (IAPS): Affective ratings of pictures and instruction manual. In.

Lange J, Oostenveld R, Fries P (2013) Reduced occipital alpha power indexes enhanced excitability rather than improved visual perception. J Neurosci 33:3212-3220.

Lanius RA, Frewen PA, Tursich M, Jetly R, McKinnon MC (2015) Restoring large-scale brain networks in PTSD and related disorders: a proposal for neuroscientifically-informed treatment interventions. Eur J Psychotraumatol 6:27313.

Lanius RA, Bluhm RL, Coupland NJ, Hegadoren KM, Rowe B, Theberge J, Neufeld RW, Williamson PC, Brimson M (2010) Default mode network connectivity as a predictor of post-traumatic stress disorder symptom severity in acutely traumatized subjects. Acta Psychiatr Scand 121:33-40.

Laufs H, Krakow K, Sterzer P, Eger E, Beyerle A, Salek-Haddadi A, Kleinschmidt A (2003) Electroencephalographic signatures of attentional and cognitive default modes in spontaneous brain activity fluctuations at rest. Proc Natl Acad Sci U S A 100:11053-11058.

Lehtela L, Salmelin R, Hari R (1997) Evidence for reactive magnetic 10-Hz rhythm in the human auditory cortex. Neurosci Lett 222:111-114.

Li W (2019) Perceptual Mechanisms of Anxiety and Its Disorders. In: Cambridge Handbook of Anxiety and Related Disorders (Olatunji B, ed): Cambridge Press.

Liberzon I, Abelson JL (2016) Context Processing and the Neurobiology of Post-Traumatic Stress Disorder. Neuron 92:14-30.

Liu Q, Farahibozorg S, Porcaro C, Wenderoth N, Mantini D (2017) Detecting large-scale networks in the human brain using high-density electroencephalography. Hum Brain Mapp 38:4631-4643.

Llinas RR, Ribary U, Jeanmonod D, Kronberg E, Mitra PP (1999) Thalamocortical dysrhythmia: A neurological and neuropsychiatric syndrome characterized by magnetoencephalography. Proc Natl Acad Sci U S A 96:15222-15227.

Mantini D, Perrucci MG, Del Gratta C, Romani GL, Corbetta M (2007) Electrophysiological signatures of resting state networks in the human brain. Proc Natl Acad Sci U S A 104:13170-13175.

Menon V (2011) Large-scale brain networks and psychopathology: a unifying triple network model. Trends Cogn Sci 15:483-506.

Menon V, Uddin LQ (2010) Saliency, switching, attention and control: a network model of insula function. Brain Struct Funct 214:655-667.

Miller DR, Hayes SM, Hayes JP, Spielberg JM, Lafleche G, Verfaellie M (2017a) Default Mode Network Subsystems are Differentially Disrupted in Posttraumatic Stress Disorder. Biol Psychiatry Cogn Neurosci Neuroimaging 2:363-371.

Miller DR, Logue MW, Wolf EJ, Maniates H, Robinson ME, Hayes JP, Stone A, Schichman S, McGlinchey RE, Milberg WP, Miller MW (2017b) Posttraumatic stress disorder symptom severity is associated with reduced default mode network connectivity in individuals with elevated genetic risk for psychopathology. Depress Anxiety 34:632-640.

642 Mo J, Liu Y, Huang H, Ding M (2013) Coupling between visual alpha oscillations and default mode
643 activity. Neuroimage 68:112-118.
644 Mobascher A, Brinkmeyer J, Warbrick T, Musso F, Wittsack HJ, Stoermer R, Saleh A, Schnitzler A,
645 Winterer G (2009) Fluctuations in electrodermal activity reveal variations in single trial brain
646 responses to painful laser stimuli--a fMRI/EEG study. Neuroimage 44:1081-1092.
647 Morgan CA, 3rd, Grillon C (1999) Abnormal mismatch negativity in women with sexual assault-related
648 posttraumatic stress disorder. Biol Psychiatry 45:827-832.
649 Mueller-Pfeiffer C, Schick M, Schulte-Vels T, O'Gorman R, Michels L, Martin-Soelch C, Blair JR, Rufer M,
650 Schnyder U, Zeffiro T, Hasler G (2013) Atypical visual processing in posttraumatic stress disorder.
651 Neuroimage Clin 3:531-538.
652 Mulert C, Jager L, Schmitt R, Bussfeld P, Pogarell O, Moller HJ, Juckel G, Hegerl U (2004) Integration of
653 fMRI and simultaneous EEG: towards a comprehensive understanding of localization and time-
654 course of brain activity in target detection. Neuroimage 22:83-94.
655 Neuner I, Arrubla J, Werner CJ, Hitz K, Boers F, Kawohl W, Shah NJ (2014) The default mode network and
656 EEG regional spectral power: a simultaneous fMRI-EEG study. PLoS One 9:e88214.
657 Neylan TC, Fletcher DJ, Lenoci M, McCallin K, Weiss DS, Schoenfeld FB, Marmar CR, Fein G (1999)
658 Sensory gating in chronic posttraumatic stress disorder: reduced auditory P50 suppression in
659 combat veterans. Biol Psychiatry 46:1656-1664.
660 Nicholson AA, Friston KJ, Zeidman P, Harricharan S, McKinnon MC, Densmore M, Neufeld RWJ, Theberge
661 J, Corrigan F, Jetly R, Spiegel D, Lanius RA (2017) Dynamic causal modeling in PTSD and its
662 dissociative subtype: Bottom-up versus top-down processing within fear and emotion regulation
663 circuitry. Hum Brain Mapp 38:5551-5561.
664 Nolan H, Whelan R, Reilly RB (2010) FASTER: Fully Automated Statistical Thresholding for EEG artifact
665 Rejection. J Neurosci Methods 192:152-162.
666 Olbrich S, Mulert C, Karch S, Trenner M, Leicht G, Pogarell O, Hegerl U (2009) EEG-vigilance and BOLD
667 effect during simultaneous EEG/fMRI measurement. Neuroimage 45:319-332.
668 Palva S, Palva JM (2007) New vistas for alpha-frequency band oscillations. Trends Neurosci 30:150-158.
669 Pascual-Marqui RD, Lehmann D, Koukkou M, Kochi K, Anderer P, Saletu B, Tanaka H, Hirata K, John ER,
670 Prichep L, Biscay-Lirio R, Kinoshita T (2011) Assessing interactions in the brain with exact low-
671 resolution electromagnetic tomography. Philos Trans A Math Phys Eng Sci 369:3768-3784.
672 Pizzagalli DA, Oakes TR, Fox AS, Chung MK, Larson CL, Abercrombie HC, Schaefer SM, Benca RM,
673 Davidson RJ (2004) Functional but not structural subgenual prefrontal cortex abnormalities in
674 melancholia. Mol Psychiatry 9:325, 393-405.
675 Raichle ME, MacLeod AM, Snyder AZ, Powers WJ, Gusnard DA, Shulman GL (2001) A default mode of
676 brain function. Proc Natl Acad Sci U S A 98:676-682.
677 Rauch SL, Shin LM, Phelps EA (2006) Neurocircuitry models of posttraumatic stress disorder and
678 extinction: human neuroimaging research--past, present, and future. Biol Psychiatry 60:376-382.
679 Ros T, Theberge J, Frewen PA, Kluetsch R, Densmore M, Calhoun VD, Lanius RA (2013) Mind over
680 chatter: plastic up-regulation of the fMRI salience network directly after EEG neurofeedback.
681 Neuroimage 65:324-335.
682 Sadaghiani S, Scheeringa R, Lehongre K, Morillon B, Giraud AL, Kleinschmidt A (2010) Intrinsic
683 connectivity networks, alpha oscillations, and tonic alertness: a simultaneous
684 electroencephalography/functional magnetic resonance imaging study. J Neurosci 30:10243-
685 10250.
686 Samogin J, Liu Q, Marino M, Wenderoth N, Mantini D (2019) Shared and connection-specific intrinsic
687 interactions in the default mode network. Neuroimage 200:474-481.
688 Scheeringa R, Petersson KM, Kleinschmidt A, Jensen O, Bastiaansen MCM (2012) EEG alpha power
689 modulation of fMRI resting-state connectivity. Brain connectivity 2:254-264.

690 Schulman JJ, Cancro R, Lowe S, Lu F, Walton KD, Llinas RR (2011) Imaging of thalamocortical dysrhythmia
691 in neuropsychiatry. Front Hum Neurosci 5:69.
692 Seeley WW, Menon V, Schatzberg AF, Keller J, Glover GH, Kenna H, Reiss AL, Greicius MD (2007)
693 Dissociable intrinsic connectivity networks for salience processing and executive control. J
694 Neurosci 27:2349-2356.
695 Spielberg JM, McGlinchey RE, Milberg WP, Salat DH (2015) Brain network disturbance related to
696 posttraumatic stress and traumatic brain injury in veterans. Biol Psychiatry 78:210-216.
697 Sripada RK, King AP, Welsh RC, Garfinkel SN, Wang X, Sripada CS, Liberzon I (2012) Neural dysregulation
698 in posttraumatic stress disorder: evidence for disrupted equilibrium between salience and
699 default mode brain networks. Psychosomatic medicine 74:904.
700 Stewart LP, White PM (2008) Sensory filtering phenomenology in PTSD. Depress Anxiety 25:38-45.
701 Tamber-Rosenau BJ, Dux PE, Tombu MN, Asplund CL, Marois R (2013) Amodal processing in human
702 prefrontal cortex. J Neurosci 33:11573-11587.
703 Tang AC, Sutherland MT, Sun P, Zhang Y, Nakazawa M, Korzekwa A, Yang Z, Ding M (2007) Top-Down
704 Versus Bottom-Up Processing in the Human Brain: Distinct Directional Influences Revealed by
705 Integrating SOBI and Granger Causality. In: Independent Component Analysis and Signal
706 Separation: 7th International Conference, ICA 2007, London, UK, September 9-12, 2007.
707 Proceedings (Davies ME, James CJ, Abdallah SA, Plumbley MD, eds), pp 802-809. Berlin,
708 Heidelberg: Springer Berlin Heidelberg.
709 Teicher MH, Samson JA, Anderson CM, Ohashi K (2016) The effects of childhood maltreatment on brain
710 structure, function and connectivity. Nat Rev Neurosci 17:652-666.
711 Thatcher RW, North DM, Biver CJ (2014) LORETA EEG phase reset of the default mode network. Front
712 Hum Neurosci 8:529.
713 Uhlhaas PJ, Haenschel C, Nikolic D, Singer W (2008) The role of oscillations and synchrony in cortical
714 networks and their putative relevance for the pathophysiology of schizophrenia. Schizophr Bull
715 34:927-943.
716 Vanneste S, Song JJ, De Ridder D (2018) Thalamocortical dysrhythmia detected by machine learning. Nat
717 Commun 9:1103.
718 Vitacco D, Brandeis D, Pascual-Marqui R, Martin E (2002) Correspondence of event-related potential
719 tomography and functional magnetic resonance imaging during language processing. Hum Brain
720 Mapp 17:4-12.
721 Wang C, Rajagovindan R, Han SM, Ding M (2016) Top-Down Control of Visual Alpha Oscillations: Sources
722 of Control Signals and Their Mechanisms of Action. Front Hum Neurosci 10:15.
723 Whitton AE, Deccy S, Ironside ML, Kumar P, Beltzer M, Pizzagalli DA (2018) Electroencephalography
724 Source Functional Connectivity Reveals Abnormal High-Frequency Communication Among
725 Large-Scale Functional Networks in Depression. Biol Psychiatry Cogn Neurosci Neuroimaging
726 3:50-58.
727 Worrell GA, Lagerlund TD, Sharbrough FW, Brinkmann BH, Busacker NE, Cicora KM, O'Brien TJ (2000)
728 Localization of the epileptic focus by low-resolution electromagnetic tomography in patients
729 with a lesion demonstrated by MRI. Brain Topogr 12:273-282.
730 Yeo BT, Krienen FM, Sepulcre J, Sabuncu MR, Lashkari D, Hollinshead M, Roffman JL, Smoller JW, Zollei L,
731 Polimeni JR, Fischl B, Liu H, Buckner RL (2011) The organization of the human cerebral cortex
732 estimated by intrinsic functional connectivity. J Neurophysiol 106:1125-1165.
733 Zhang W, Hashemi MM, Kaldewaij R, Koch SBJ, Beckmann C, Klumpers F, Roelofs K (2019) Acute stress
734 alters the 'default' brain processing. Neuroimage 189:870-877.
735 Zumsteg D, Friedman A, Wennberg RA, Wieser HG (2005) Source localization of mesial temporal
736 interictal epileptiform discharges: correlation with intracranial foramen ovale electrode
737 recordings. Clin Neurophysiol 116:2810-2818.

738 **Table 1 Participant Demographics**

	PTSD	Controls
Age (years)	34.6 ± 10.4	31.1 ± 13.1
Gender (female/male)	16/9	25/19
Substance Use (%) †	64%*	7.5%
Medication Use (%)	40%	36%
PCL Total	61.0 ± 16.1*	37.6 ± 13.4
PCL-Hypervigilance	4.1 ± 1.0*	2.1 ± 1.2
BAI	26.2 ± 15.7*	11.8 ± 9.4
BDI	26.8 ± 12.5*	17.4 ± 9.7

739 PCL = Posttraumatic Stress Disorder Checklist, BAI = Beck Anxiety Inventory, BDI = Beck

740 Depression Inventory; † = Subjects with opioid, stimulant, and cocaine use were excluded. * $p <$

741 0.005.

Table 2 Summary of Group Effects

Effects *(PTSD < Control)*	***State***	Visual cortex	DMN
Alpha power	***S-RS***	Cun., Precun., Sup. Occ.	PCC
	M-RS	Precun.	PCC, mPFC
	M-RS - S-RS	*n. s.*	*n. s.*
Alpha GC	***S-RS***	*n. s.*	*PCC→VC*
	M-RS	VC→PCC, *VC→mPFC*	PCC→mPFC
	M-RS - S-RS	VC→PCC, VC→mPFC	*n. s.*

Cun = cuneus; Precun = precuneus; Sup. Occ. = superior occipital gyrus; VC = visual cortex. *Italicized ones* were significant ($p < 0.05$) before multiple-comparison correction; all other effects survived correction.

Table 3 Summary of Individual Group Contrasts

	Contrast	S-RS	M-RS	M-RS – S-RS
Alpha Power	PTSD vs. HC	PCC/Precun. (20, -60, 35) *(t = -3.00; k = 71)* Cun./SOC (45, -80, 25) *(t = -3.42; k = 71)* R. Insula (35, -5, 15) *(t = -3.18; k = 10)*	PCC/Precun. (5, -55, 50) *(t = -2.41; k = 121)* mPFC (10, 65, 0) *(t = -2.87; k = 10)* R. Insula (45, -5, 15) *(t = -2.98; k = 10)*	*n.s.*
	PTSD vs. GAD	PCC/Precun. (15, -50, 40) *(t = -3.31; k = 112)* Cun. (5, -65, 15) *(t = -2.88; k = 112)* L. Insula (-30, 25, 0) *(t = -4.29; k = 30)*	PCC/Precun. (15, -45, 40) *(t = -3.31; k = 102)* mPFC (-15, 65, -15) *(t = -3.31; k = 95)* R./L. Insula (60, -15, 30/ -30, 25, 5) *(t = -3.96/-3.58; k = 64/65)*	*n.s.*
Alpha Connectivity	PTSD vs. HC	PCC→VC* *(t = -1.72, p = 0.046)*	PCC→mPFC *(t = -2.68, p = 0.010)* VC→PCC *(t = -2.36, p = 0.023)*	VC→PCC* (*t* = -1.87, *p* = 0.034)
	PTSD vs. GAD	PCC→VC* *(t = -1.83, p = 0.037)*	PCC→mPFC *(t = -2.68, p = 0.010)* VC→PCC *(t = -3.30, p = 0.002)* mPFC→PCC *(t = -3.25, p = 0.003)*	VC→PCC* (*t* = -1.87, *p* = 0.035) VC→mPFC (*t* = -2.29, *p* = 0.027)

All effects survived FDR $p < .05$. * = one-tailed. Peak MNI coordinates (X, Y, Z) are provided, along with cluster sizes (k). SOC = Superior Occipital Gyrus; R/L = right/left.

FIGURE LEGENDS

Figure 1. Group differences in alpha power. (A) During the S-RS, the PTSD group demonstrated reduced alpha power in the visual cortex (the cuneus, precuneus, and superior occipital gyrus), the posterior DMN hub (PCC), and anterior and posterior insula. (B) During the M-RS, the PTSD group showed reduced alpha power in the visual cortex (the cuneus and precuneus), both the anterior and posterior DMN hubs (mPFC and PCC), and anterior and posterior insula. Cun = cuneus; Precun = precuneus; AI = anterior insula; PI = posterior insula; Sup. Occ. = superior occipital gyrus.

Figure 2. Group differences in alpha connectivity. Left column: matrices of group differences PTSD minus Controls) in directed alpha-frequency connectivity (GC) showed (A) reduced PCC→VC alpha connectivity (albeit not FDR corrected) during the S-RS; and (B) reduced PCC→mPFC alpha connectivity during the M-RS and, as enclosed in a red box, more reduction from the S-RS to the M-RS in VC→PCC and VC→mPFC alpha connectivity. Right column: schematic presentations of group-differences in connectivity during the S-RS (A) and M-RS (B), with solid and dotted arrows reflecting connections surviving and not surviving FDR correction, respectively. Arrows in light blue and dark blue reflect significant effects from simple group contrasts and double contrasts of State and Group, respectively. Our discussion focused on the effects surviving the multiple comparison correction. *$p < 0.05$; **$p < 0.01$; † $p < 0.1$; white * = FDR corrected; gray * = not FDR corrected. VC = visual cortex.

Figure 3. Whole-brain PCC connectivity maps during the M-RS. Connectivity for all Brodmann areas (BAs) with the PCC as the Sender and Receiver ($p < .05$). Only the PCC→BA 22 connectivity (dark red) survived whole-brain correction (FWE $p = .0006$).

781

782 **Figure 4. Clinical associations between alpha power and hypervigilance.** Whole-brain
783 correlation maps of alpha power and hypervigilance indicated negative correlations in both the
784 dorsal (i.e., SPL, Precuneus) and ventral (i.e., ITG) visual cortices during the S-RS (A) and both
785 DMN hubs (mPFC and PCC) during the M-RS (B). SPL = superior parietal lobule; ITG =
786 inferior temporal gyrus.

787

788 **Figure 1.**

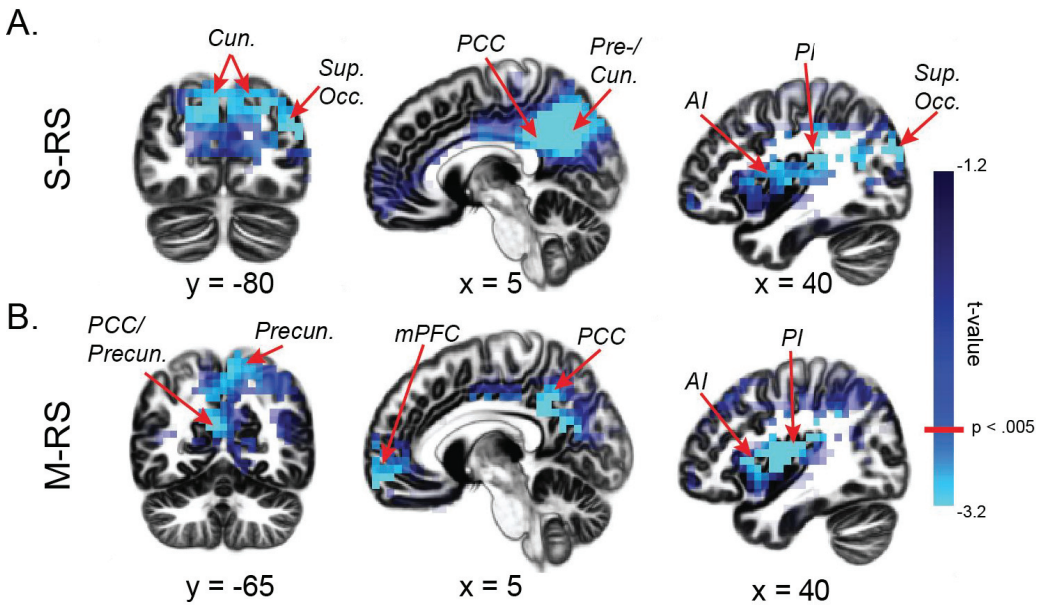

789

Figure 2.

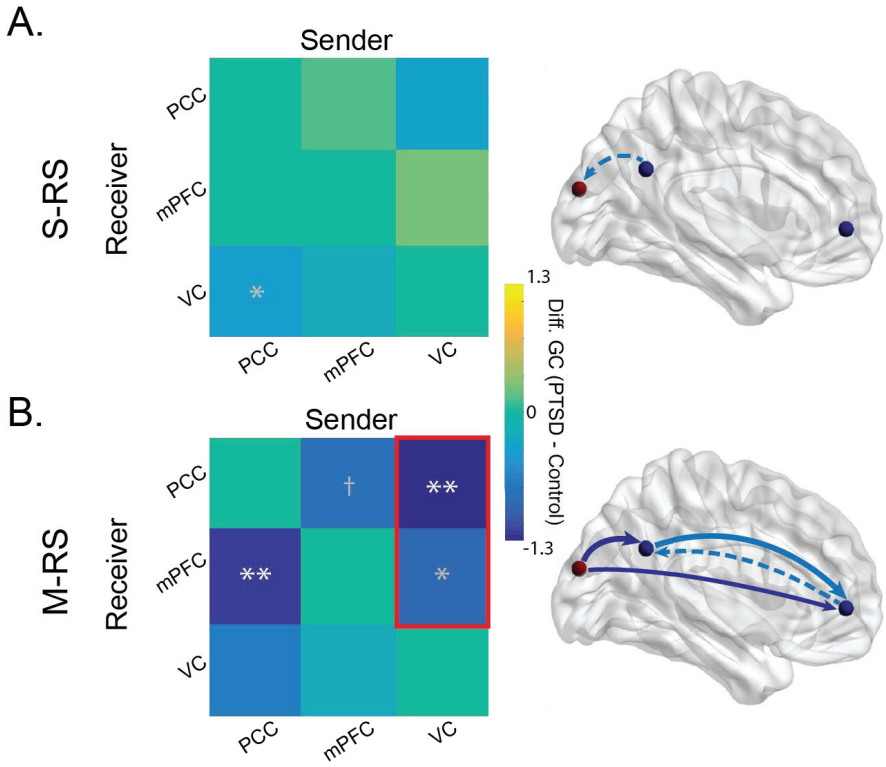

Figure 3.

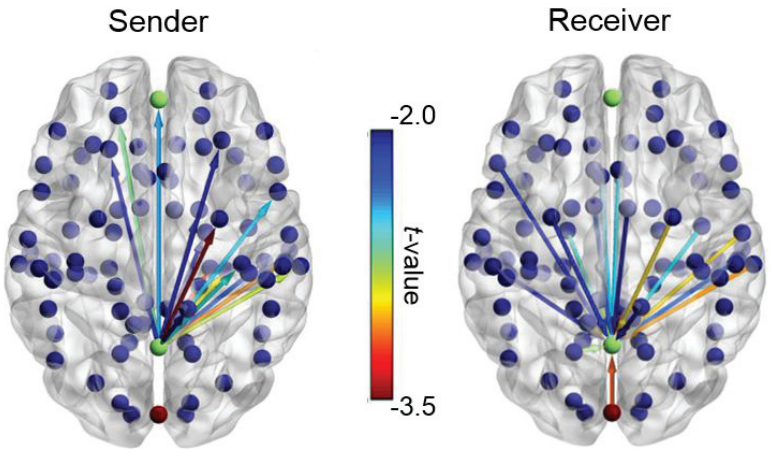

795 **Figure 4.**

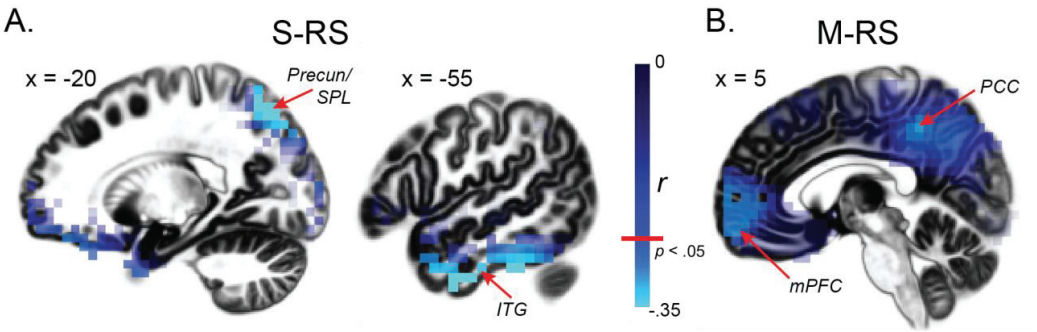

796

797